American Mineralogist, Volume 67, pages 1–13, 1982

Petrology and geochemistry of calc-alkaline andesite of presumed upper mantle origin from Itinome-gata, Japan

KEN-ICHIRO AOKI AND HIROKAZU FUJIMAKI

Institute of Mineralogy, Petrology and Economic Geology
Tohoku University, Sendai 980, Japan

Abstract

Itinome-gata and Sannome-gata volcanoes, northeastern Japan, are characterized by the eruption of mafic to salic andesite of the calc-alkaline series and high-alumina basalt, both of which contain small amounts of high-pressure diopside and forsterite megacrysts, lherzolite and websterite derived from the upper mantle, and gabbro and amphibolite xenoliths from the lower crust (about 20 to 30 km in depth). It seems likely that this is the first discovery of upper mantle peridotite xenoliths in calc-alkaline andesite. This andesite is characterized by presence of hornblende and biotite phenocrysts.

Three representative basalts and five andesites have been analyzed for major elements by a conventional method, and for rare earth elements and Ba by the isotope dilution method.

Major element variations of the basalt and andesite suite follow a typical calc-alkaline trend with increasing fractionation. In addition, there are no essential differences of Ba and REE concentrations and chondrite-normalized patterns between them. Furthermore, Sr^{87}/Sr^{86} ratios in basalt and the most salic andesite are nearly the same (0.7030 and 0.7033, respectively).

It is possible to conclude that the andesite magmas are produced by fractional crystallization of basalt magma based on mineral assemblages, major element variations and strontium isotope ratios. However, REE and Ba concentrations and patterns are not consistent with this hypothesis. Accordingly, it is more probable that andesite and basalt magmas are formed independently by nearly the same degree of partial melting of hydrous and less hydrous parts of upper mantle peridotite, with increasing temperature, at the depths of 40 to 60 km.

Introduction

Recently, much attention has been paid to the origin of andesites of the calc-alkaline series, which are widely distributed in time and space in island arcs and continental margins. Several new hypotheses have been proposed on the basis of the results of experimental petrology and geochemistry (*cf.* Allen *et al.*, 1972; Kushiro *et al.*, 1968; Green and Ringwood, 1968; Boettcher, 1973; Ringwood, 1974). These include formation of andesite magma by (1) partial melting of hydrous mantle peridotite, (2) partial melting of subducted oceanic crust, (3) magma mixing and (4) amphibole fractionation of basaltic magma. However, it is very difficult to find direct evidence to evaluate these proposals.

Itinome-gata volcano in northeastern Japan is one of the most famous localities of upper mantle and lower crustal fragments in Japan (Fig. 1). A large variety of xenolith types has been studied by many investigators (Kuno, 1967; Kuno and Aoki, 1970; Aoki, 1971; Aoki and Shiba, 1973a, b, 1974a, b; Takahashi, 1978, 1980; Zashu *et al.*, 1980; Tanaka and Aoki, 1981), though detailed petrographic and geochemical studies of host rocks have been neglected. Recently, Katsui and Nemoto (1977) and Katsui *et al.* (1979) carried out field work in the Itinome-gata district and found that the xenolith-bearing volcanic rocks are calc-alkaline andesite at Itinome-gata and silica-undersaturated basalt at Sannome-gata.

Our purpose in this paper is to describe the mineralogy, petrography and REE geochemistry of high-alumina basalt and calc-alkaline andesite from the Itinome-gata district and to discuss the origin of these rocks.

0003–004X/82/0102–0001$02.00

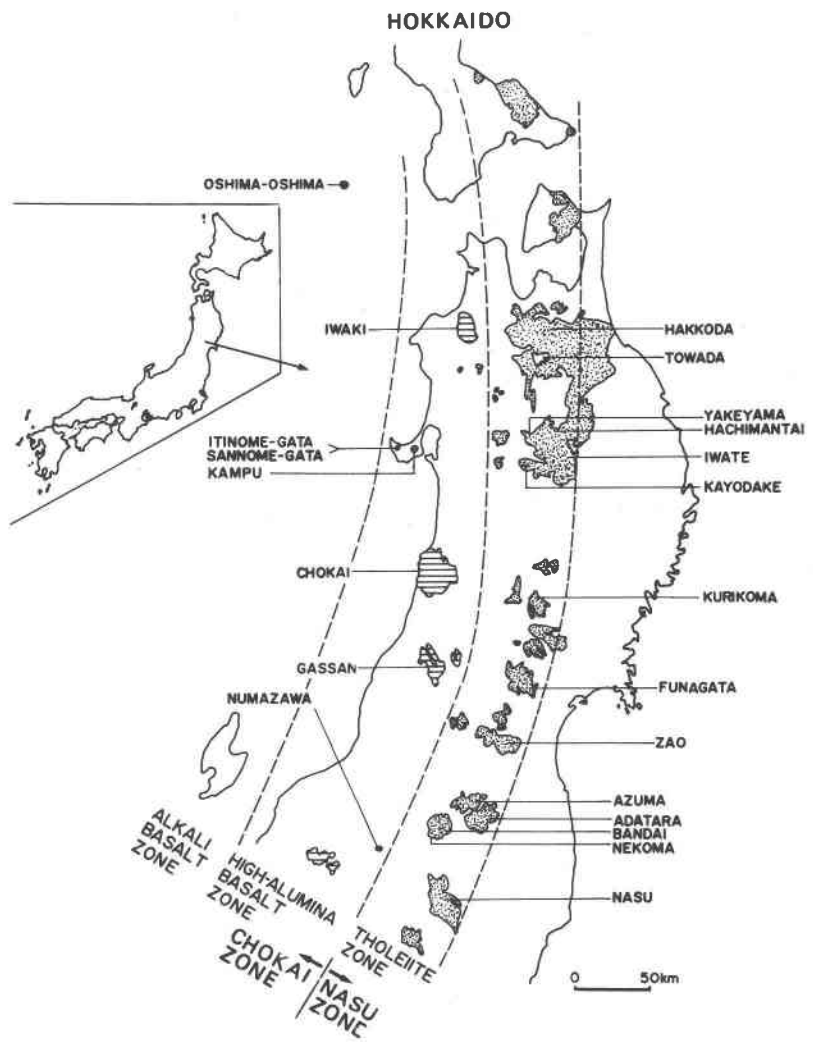

Fig. 1. Map showing the location of Itinome-gata and Sannome-gata, northeastern Japan.

Occurrence and petrography

Three maars or craters, Itinome-gata, Ninome-gata and Sannome-gata, all of which formed about 10,000 years ago, are located on the west coast of northeastern Japan (Fig. 1). The basement underlying the Itinome-gata district consists of a complex of Cretaceous to Paleogene salic plutonic and volcanic rocks and Neogene volcanics and sediments. According to the field work of Katsui *et al.* (1979), eruption took place in three distinct stages separated by intercalated soil zones. The first stage began with the destruction of near-surface rocks and opening of the Itinome-gata and Ninome-gata vents by steam explosions. This activity was followed by the eruption of gray- to white-colored andesitic pumices and abundant accidental upper crustal fragments, which are represented by mud flow and base-surge deposits. All xenoliths derived from the upper mantle and lower crust occur as ellipsoidal bombs or as loose blocks, within the andesitic pumices, up to 30 cm in diameter. Megacrysts of diopside (less than 5 cm in size), which may contain euhedral forsterite crystals, occur also as crystal lapilli or as "xenocrysts" in the host rocks. In the third stage, basaltic scoria falls were erupted from the Sannome-gata crater; these also contain small amounts of deep-seated xenoliths.

Basalt scoria from Sannome-gata usually shows a porphyritic appearance due to the presence of abundant quartz and feldspar xenocrysts derived from granitic basement rocks. Under the microscope, the commonest phenocrysts are olivines, which occupy less than 5% by volume, and range up to 0.8 mm in

length but are mostly less than 0.4 mm. They are euhedral tabular or elongated parallel to the *c* crystallographic axis, showing weak zoning at the peripheral margins of each crystal. Clinopyroxene phenocrysts are much less common than those of olivine, being subhedral, short, and prismatic in form and up to 0.3 mm in length. Weak sector zoning is always seen. The groundmass is rather fine-grained and hypocrystalline with numerous vesicles. It consists of brown glass, plagioclase laths, subhedral clinopyroxene, and euhedral olivine, in decreasing order of abundance. Plagioclase xenocrysts have an irregular anhedral form, up to 3 mm in size. All of the crystals of plagioclase show mottled appearance due to glass inclusions in the margins, and are always immediately surrounded by calcic rims of groundmass plagioclase composition. Quartz xenocrysts are irregular in crystal outline. They are surrounded by thin rims composed of minute acicular clinopyroxene. Olivine xenocrysts, presumably derived from dispersed peridotite, are sometimes recognized. They are irregular in form, less than 3 mm in grain size, and invariably homogeneous. Accordingly, it is very easy to distinguish between phenocrystic and xenocrystic olivines by their grain size and crystal form.

Andesite pumices are megascopically gray in mafic rocks to white in salic rocks and show a porphyritic appearance which is due to the presence of abundant quartz and plagioclase xenocrysts. Phenocrystic minerals are plagioclase (up to 4 mm in size), olivine (0.6 mm), clinopyroxene (0.8 mm), green hornblende (1 mm), biotite (2 mm) and magnetite (0.5 mm). The modal volume of olivine and clinopyroxene gradually decrease and these of hornblende and biotite increase with increasing SiO_2 content. In addition to these minerals, small amounts of quartz (0.5 mm) and apatite are found as phenocrysts in salic rocks. All of the andesites contain small to negligible amounts of mafic xenocrysts derived from the upper mantle and lower crust. The mafic phenocrysts can be distinguished from xenocrysts by their crystal outline: the former are euhedral and smaller in size, while the latter are irregular, broken and homogeneous. No phenocrystic or groundmass orthopyroxenes have been identified in any basalts and andesites.

Chemistry

Analytical methods and results

Because all the rocks contain abundant xenocrysts, it is difficult to interpret whole rock analyses. Therefore, scoriaceous and pumiceous samples were carefully crushed to pass through a 48- or 100-mesh sieve. They were washed with distilled water and dried. Most xenocrysts and phenocrysts separate easily from the soft and loose groundmass. The groundmass was separated in the Frantz isodynamic separator. Finally, the light fraction (specific gravity is less than 2.5) was floated on diluted methylene iodide. The most salic pumice with less abundance of accidental fragments was purified by elimination of impurities under the binocular microscope.

Major element compositions were determined by wet chemical methods for silicate analysis combined with flame photometric and atomic absorption spectroscopic techniques. Mineral analyses were done on a Hitachi scanning electron-probe microanalyzer, Model X-560S, using an energy-dispersive analytical system (Kevex Corporation). Synthetic and natural minerals were used as standards. Detailed procedures and accuracy of analysis by the energy-dispersive analytical system are given by Fujimaki and Aoki (1980).

The determination of Ba and rare earth elements (REE) was made by the technique of stable isotope dilution using a JMS-05RB type, 30 cm radius mass spectrometer of the Geological Survey of Japan. Precision of the analysis is better than 2 percent. Analytical data are shown in Tables 1 to 3.

Rock composition

The rocks show a restricted range in major element composition. SiO_2 contents range from 51 to 61 percent, and the other components gradually increase or decrease systematically with SiO_2 variation. Comparing the basalts from Itinome-gata district with those from other localities of Japan, the former exhibit characteristics intermediate between typical tholeiites and alkali basalts and resemble high-alumina basalts from Izu-Hakone region (Kuno, 1960). They are characterized by rather high Al_2O_3, MgO, and total alkalies and low total FeO. In detail however, there are differences which may be significant. Most high-alumina basalts have K_2O contents of less than 0.8%. The average Itinome-gata basalt composition has a higher K_2O content of 1.3% comparable to that of alkali basalts from southwest Japan.

Although these basalts contain neither normative quartz nor nepheline (normalizing Fe_2O_3/FeO + Fe_2O_3 to 0.2–0.15), all of the andesites are saturated in silica, and show many similarities with typical

Table 1. Chemical analyses and norms (water-free basis) of xenolith-bearing basalts and andesites from Itinome-gata district

	1	2	3	4	5	6	7	8	9
SiO_2	50.95	59.72	50.55	53.87	54.65	58.84	59.29	59.73	60.65
TiO_2	0.96	1.04	1.06	0.89	0.72	0.71	0.71	0.61	1.12
Al_2O_3	16.76	17.02	17.20	16.19	18.74	16.35	16.59	16.68	16.41
Fe_2O_3	2.21	1.92	2.58	3.07	2.44	2.43	2.51	1.65	1.73
FeO	5.99	6.12	5.85	4.77	3.80	3.40	3.21	3.01	2.81
MnO	0.18	0.18	0.19	0.13	0.25	0.16	0.16	0.15	0.15
MgO	8.25	7.84	6.82	6.41	4.50	3.37	3.52	3.45	3.36
CaO	9.53	9.56	9.59	8.44	7.04	7.22	6.69	5.27	5.57
Na_2O	2.58	2.66	2.46	2.52	3.10	2.86	3.13	3.19	3.38
K_2O	1.31	1.30	1.43	1.93	2.01	2.70	2.58	2.97	2.29
H_2O	0.88	0.99	1.80	0.96	2.27	1.38	1.33	2.38	2.05
P_2O_5	0.20	0.19	0.21	0.31	0.24	0.16	0.16	0.31	0.29
Total	99.80	99.54	99.74	99.49	99.76	99.58	99.88	99.40	99.81
Q			0.54	5.60	6.50	12.94	12.76	13.47	16.13
Or	7.79	7.79	8.63	11.58	12.19	16.25	15.47	18.09	13.80
Ab	22.07	22.86	21.23	21.65	26.90	24.59	26.90	27.84	29.26
An	30.62	31.10	32.35	27.56	32.07	24.25	23.93	23.09	23.39
Di Wo	6.62	6.61	6.19	5.39	0.88	4.68	3.66	0.72	1.23
Di En	4.43	4.33	4.28	3.76	0.59	3.10	2.52	0.48	0.88
Di Fs	1.70	1.82	1.41	1.17	0.22	1.24	0.84	0.18	0.24
Hy En	12.64	10.94	13.05	12.45	10.91	5.44	6.36	8.38	7.68
Hy Fs	4.88	4.63	5.95	3.89	4.13	2.19	2.15	3.34	1.99
Ol Fo	2.60	3.19							
Ol Fa	1.11	1.48							
Mt	3.24	2.82	3.82	4.51	3.63	3.59	4.02	2.48	2.50
Il	1.84	2.02	2.05	1.71	1.41	1.37	1.37	1.20	2.19
Ap	0.47	0.44	0.50	0.74	0.61	0.37	0.37	0.77	0.71

1. Groundmass of augite-bearing olivine basalt (7772901)
2. Groundmass of augite-bearing olivine basalt (7772901')
3. Groundmass of augite-bearing olivine basalt (7790302)
4. Groundmass of hornblende biotite augite olivine andesite (7790303)
5. Groundmass of olivine augite biotite hornblende andesite (7790304)
6. Groundmass of augite, olivine and quartz-bearing biotite hornblende andesite (7790301)
7. Groundmass of augite, olivine and quartz-bearing biotite hornblende andesite (7790305)
8. Groundmass of olivine, augite and quartz-bearing hornblende biotite andesite (7772710)
9. Olivine, augite and quartz-bearing hornblende biotite andesite (7772710), whole rock analysis

Nos. 1 -3: Scoria from Sannome-gata, Nos. 4 - 9: Pumice from Itinome-gata.

calc-alkaline andesites from island arcs or continental margins.

In Figure 2, the variation of main oxides against SiO_2 contents of basalts and andesites is plotted along with the average variation curve of volcanic rocks of the Chokai zone (high-alumina basalt zone). The Itinome-gata volcano is a part of this volcanic zone of northeastern Japan (Fig. 1). Total FeO, MgO and CaO decrease gradually from basalt to salic andesite while Na_2O and K_2O increase, and it is noticeable that the basalt–andesite suite of the Itinome-gata district is clearly higher in MgO and K_2O and lower in total FeO and Na_2O than the average curves.

The data are also plotted in a MFA [MgO–(FeO + Fe_2O_3)–(Na_2O + K_2O)] diagram (Fig. 3) together with the fractionation trends of the tholeiitic series and calc-alkaline series of Nasu zone (outer volcanic zone), northeastern Japan. All the rocks plot below the fields of the calc-alkaline series of Nasu zone in spite of being in the same rock series, and consequently trend from the MgO–(FeO + Fe_2O_3) side line toward the apex of alkalies, following the typical course of island arc calc-alkaline series.

REE and Ba

Chondrite-normalized Ba and REE patterns for one whole rock and eight groundmass analyses from the Itinome-gata district are shown in Figure 4. It is emphasized that none of the patterns are correlated with either SiO_2 or K_2O contents. The very marked enrichment of light REE (Sm to La) is notable and the rocks are essentially indistinguishable from one another, showing the typical abundances found in calc-alkaline rocks (Jakes and Gill, 1970). Total REE abundances and La/Yb ratios in these rocks vary from 98 ppm to 118 ppm and 7.1 to 9.1 respectively, with weak negative anomalies evident in only three patterns. There is a slight difference between patterns of the most salic andesite and its groundmass (Nos. 9 and 8, Fig. 4); the former shows weak positive Eu anomaly due to accumulation of some plagioclase phenocrysts.

Plagioclases

The compositional range of groundmass plagioclase in the basalts is $An_{79.4}Ab_{20.3}Or_{0.3}$ to $An_{68}Ab_{31}Or_1$ whereas the cores and narrow margins of plagioclase phenocrysts in the andesites are $An_{65}Ab_{33}Or_2$ to $An_{32}Ab_{63}Or_5$. It is clear that the most sodic margins of the former are still less sodic than the cores of the latter. The compositions of the cores of phenocrysts tend to be more sodic with increase in SiO_2 content of the host rocks, but the sodic margins are not strikingly different from one another. The Or content increases from 0.3 to 6.9 with increase in the Ab content (Fig. 5).

Olivines

Phenocrystic olivines in the basalts and andesites range in composition from cores of $Fo_{88.3}$ and $Fo_{90.2}$ to rims of $Fo_{84.2}$ and $Fo_{82.3}$ respectively, and euhedral olivine in diopside megacrysts from the andesite is $Fo_{87.3}$. On the other hand, groundmass olivines in basalts are $Fo_{86.4}$ to $Fo_{78.5}$. All the olivines are characterized by very high Fo contents and a narrow compositional range, regardless of their occurrence and bulk rock composition (Fig. 6). As previously mentioned, basalts and andesites con-

Table 2. Ba and REE abundances (ppm) in xenolith-bearing basalts and andesites from Itinome-gata district

	1	3	4	5	6	7	8	9	JB-1*	Leedey chondrite**
SiO_2 %	51	51	54	55	59	59	60	61		
Ba	1133	933	891	1175	1040	1243	1754	861	516	4.21
La	21.7	24.3	18.9	23.2	19.2	20.1	23.4	20.2	36.9	0.378
Ce	45.1	48.4	43.5	46.7	39.0	40.3	50.0	39.1	67.2	0.976
Nd	20.5	22.9	24.6	19.4	21.3	21.4	22.0	19.9	26.7	0.716
Sm	4.46	4.66	5.79	3.86	4.60	4.61	4.20	4.29	5.19	0.230
Eu	0.980	1.214	1.334	1.238	1.321	1.370	1.296	1.639	1.553	0.0866
Gd	4.65	5.19	5.37	3.93	4.00	4.05	4.20	4.42	4.81	0.311
Dy	4.74	5.01	4.67	3.93	4.14	4.58	4.70	3.92	4.18	0.390
Er	2.54	2.70	2.79	2.57	2.40	2.74	2.89	2.42	2.34	0.255
Yb	2.50	2.67	2.66	2.53	2.21	2.40	2.56	2.24	2.16	0.249
Lu	0.403	0.383	0.388	0.394	0.342	0.379	0.391	0.330	0.307	0.0387
Rb***	65.0	39					87.1			
Sr	581	469					428			
Sr^{87}/Sr^{86}	0.7030	0.7031					0.7033			

* Geological Survey of Japan geochemical standard.

** Masuda *et al.* (1973) for REE and Nakamura (1974) for Ba.

*** Zashu *et al.* (1980).

tain abundant xenocrystic olivines dispersed from upper mantle peridotite xenoliths. Accordingly, it is suggested that Mg-rich cores of phenocrysts are of xenocrystic origin, and the slightly Fe-rich margins are overgrown around the former after capture in magmas. However, there are some chemical differences between such xenocrysts and phenocrysts; the latter are poor in NiO (0.40 to 0.28 and 0.33 to 0.18%, respectively) and rich in CaO (less than 0.15 and 0.23 to 0.15%, respectively) when Fo contents are the same (Fo_{90} to Fo_{84}).

Clinopyroxenes

As is clear from Table 3 and Figure 6, clinopyroxenes show a rather wide range of composition. The cation ratios of Ca:Mg:Fe are 45.3:46.7:8.0 to 48.1:41.2:10.7 in basalt phenocrysts and 44.8:45.4:9.8 to 40.0:41.8:18.2 in andesite phenocrysts, whereas those of basalt groundmass are 47.3:41.9:10.8 to 46.9:39.2:13.8. All of the pyroxenes, like the olivines, are highly magnesian.

The most striking feature of the clinopyroxenes is the variation of Al_2O_3 (2.60–9.95%) and SiO_2 (42.78–46.93%), which are reciprocal in relation to each other. Accordingly, calculated Tschermak's components range from 5 to 18 mol percent, with the majority falling within the range 11 to 15 percent. Clinopyroxene phenocrysts can be distinguished easily from dispersed xenocrysts of peridotites by higher Al_2O_3 and total FeO and lower MgO and Cr_2O_3 in the former. High-pressure diopside megacrysts fall within the chemical range of clinopyroxene phenocrysts, but there are clear differences between them. The former are easily distinguished also from the latter by being very homogeneous, by having no perceptible zoning within a single crystal, and by their slightly Mg-rich and Ti-poor nature.

Hornblendes

Hornblendes are characterized by a wide variation of all major components except that CaO:SiO_2 and MgO tend to decrease, whereas Al_2O_3 and FeO increase with increasing SiO_2 content of the host andesites. The Mg value (100Mg/Mg + Fe + Mn ratio) shows a range from 78 to 66 in mafic andesite and 62 to 56 in salic andesite. Although these Mg values of hornblendes in andesites are clearly lower than those of pargasites in peridotite xenoliths (89 to 73), there is an overlap between hornblendes in andesites and in gabbro xenoliths; the Mg values of the latter types range from 74 to 59 (Fig. 6).

The relationships among calciferous amphibole solid solutions are graphically expressed in a Al^{IV} $-(Al^{VI} + Fe^{+3} + Cr + Ti)$ and Al^{IV}–(Na + K) diagram (Deer *et al.*, 1962). The diagram (Fig. 7)

Table 3. EPMA analyses of minerals

Olivines

	1				4			9	
	Ph-C	*Ph-M*	*Gr-C*	*Gr-M*	*Mega*	*Ph-C*	*Ph-M*	*Ph-C*	*Ph-M*
SiO_2	41.02	39.98	40.24	39.09	40.24	40.10	39.92	40.90	39.94
FeO*	11.18	14.68	12.83	17.17	11.94	13.07	15.04	9.43	15.71
MnO	0.21	0.24	0.21	0.44	0.21	0.20	0.28	0.09	0.22
MgO	48.06	44.57	46.45	42.80	47.02	46.23	44.57	48.92	44.31
NiO	0.25	0.19	0.19		0.25	0.17	0.23	0.29	
CaO	0.19	0.23	0.21	0.20	0.15	0.16	0.21	0.15	0.16
Total	100.91	99.89	99.94	99.70	99.81	99.93	100.26	99.79	100.35
Fo mol %	88.3	84.2	86.4	81.3	87.4	86.2	83.8	90.2	82.3

Clinopyroxenes

	1				4				9
	Ph-C	*Ph-M*	*Gr-C*	*Gr-M*	*Mega*	*Ph-C*	*Ph-M*	*Ph-M*	*Ph-C*
SiO_2	52.78	49.45	50.16	48.46	51.11	52.51	46.93	51.34	49.10
TiO_2	0.27	0.66	0.69	1.10	0.36	0.30	1.27	0.61	0.73
Al_2O_3	2.60	6.63	6.01	7.06	5.31	4.31	9.95	3.70	6.07
Cr_2O_3	0.41	0.26	0.42	0.17	0.11	0.13	0.14		0.16
FeO*	4.91	6.36	6.41	7.72	5.27	5.88	7.67	10.72	7.56
MnO	0.14	0.15	0.14	0.17	0.10	0.12	0.11	0.36	0.17
MgO	16.14	13.79	14.22	13.20	15.13	15.56	12.71	14.29	14.26
CaO	21.76	22.40	22.34	21.82	22.01	21.34	21.59	19.01	21.69
Na_2O	0.62	0.34	0.37	0.41	0.57	0.49	0.36	0.50	0.40
Total	99.63	100.04	100.74	100.11	99.97	100.64	100.73	100.53	100.14
Ca atom %	45.2	48.0	47.3	47.1	46.6	44.8	47.6	40.0	45.7
Mg	46.6	41.1	41.9	39.6	44.5	45.4	39.0	41.8	41.8
Fe	8.2	10.9	10.8	13.3	8.9	9.8	13.4	18.2	12.5

Plagioclases

	1		4		9	
	Gr-C	*Gr-M*	*Ph-C*	*Ph-M*	*Ph-C*	*Ph-M*
SiO_2	48.85	50.40	54.51	61.51	57.82	60.00
Al_2O_3	31.82	29.42	28.99	23.99	26.47	24.62
FeO*	0.86	0.96			0.19	0.17
CaO	16.11	14.56	11.04	6.72	9.23	6.75
Na_2O	2.28	3.64	5.02	7.03	5.88	7.60
K_2O	0.05	0.23	0.17	0.65	0.43	0.61
Total	99.79	99.21	99.73	99.90	100.03	99.76
An mol %	79.4	68.0	54.3	33.2	45.3	31.8

Hornblendes, biotites and magnetites

	4			9		
	Ho	*Bi*	*Mt*	*Ho*	*Bi*	*Mt*
SiO_2	44.05	37.30		47.53	37.35	
TiO_2	1.12	3.71	2.89	0.80	3.86	2.84
Al_2O_3	13.76	14.61	0.84	7.62	14.32	0.79
Cr_2O_3	0.17		0.20			
V_2O_3			0.38			0.35
Fe_2O_3**			61.92			61.71
FeO	9.45	17.00	31.26	14.74	17.05	31.37
MnO	0.14	0.75	2.33	1.32	0.78	1.83
MgO	15.14	13.21	0.15	12.51	13.04	0.20
CaO	11.80	0.16		11.54	0.20	
Na_2O	1.72	0.67		1.13	0.39	
K_2O	0.71	8.74		0.62	8.74	
Total	98.06	96.15	99.97	97.81	95.73	99.09
M value	72.5	57.0		58.1	56.6	
Ulvosp. mol %			8.3			8.2

* Total iron as FeO. ** Calculated as FeO and Fe_2O_3 assuming stoichiometry. *Ph;* phenocryst, *Gr;* groundmass, *C;* core *M;* margin, *Mega;* megacryst, *M value;* 100 Mg/Mg + Fe + Mn.

shows that the hornblendes in the andesites plot in the field of common hornblende, but are separated from the pargasites in peridotite and hornblende in gabbro xenoliths by their lower contents of pargasite and tschermakite molecules.

Biotites

Biotites are comparable in composition to those from common calc-alkaline andesites and dacites but have higher TiO_2 contents. The Mg values of biotites range from 59 to 54, which are the lowest among coexisting mafic silicates.

Magnetites

Homogeneous magnetite phenocrysts consist mainly of Fe_2O_3 and FeO associated with small amounts of TiO_2 and MnO. The magnetites show significant differences in composition when compared with those of calc-alkaline andesites with similar SiO content in the Nasu zone (TiO_2 14.61, Al_2O_3 2.02, Cr_2O_3 0.45, V_2O_3 1.62, Fe_2O_3 36.69, FeO 42.67, MnO 0.66, MgO 1.05, total 99.77). The former are characterized by higher Fe_2O_3 and MnO and lower TiO_2, Al_2O_3, V_2O_3, FeO and MgO, being composed of 90 mole% magnetite, 8% ulvöspinel and 2% spinel molecules; the latter magnetites consist of 55% magnetite, 41% ulvöspinel and 4% spinel.

Discussion

Tremendous amounts of calc-alkaline andesites are distributed in island arcs and continental margins. To elucidate the origin of these rocks is one of the most important problems in igneous petrology, and various hypotheses have been proposed during the past five decades. For example, andesite may represent (1) residual liquid from fractional crystallization of basalt magma (anhydrous mineral fractionation, magnetite fractionation and amphibole fractionation), (2) contamination of granitic rocks by basalt magma, (3) partial or complete melts from the lower crust, (4) basalt and salic magma mixing, (5) partial melts of oceanic crust in subduction zones, and (6) partial melts of hydrous upper mantle. In view of the large variety of mineral assemblages, mineral compositions, and bulk rock compositions among andesites, any single hypothesis cannot apply to all calc-alkaline andesite magmas. Recently, amphibole fractionation, magma mixing, partial melts of oceanic crust and partial melts of hydrous mantle peridotite have been favored by many petrologists and geochemists.

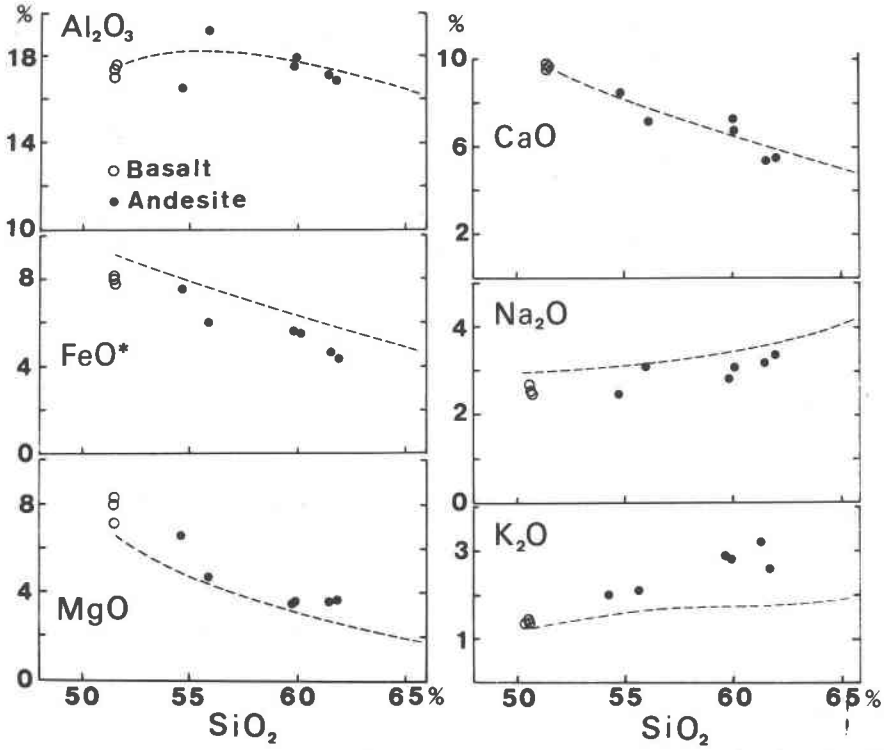

Fig. 2. Major oxides–silica variation diagram. Dashed lines are average variation curves of volcanic rocks of Chokai zone (Aoki, 1978).

First, the following petrographic and geochemical features of basalts and andesites of the Itinome-gata district must be emphasized.

1. The order of beginning of crystallization of phenocrystic minerals in the basalt–andesite suite, indicated from the mineral assemblage, crystal form, and Mg–Fe partitioning, is Mg-rich olivine → Mg-rich clinopyroxene → plagioclase → magnetite → hornblende → biotite → quartz. This crystallization sequence agrees well with that commonly observed in the calc-alkaline series except that there is no appearance of orthopyroxene, which is a common mineral in the hornblende- and biotite-free calc-alkaline series. However, hornblende- or hornblende and biotite-bearing andesite magmas, including Itinome-gata, sometimes do not have orthopyroxene at their liquidus, the reasons for which are not apparent.

2. Basalt and andesite contain upper mantle peridotite and websterite, lower crustal gabbro and amphibolite fragments, anhedral high-pressure diopside, and euhedral forsterite megacrysts. As shown by many petrologists, upper mantle peridotite xenoliths composed of olivine, enstatite, diopside and chromian spinel with or without pargasite are usually incorporated in alkali basalts and related rocks only. In extremely rare cases, olivine tholeiites include such peridotite xenoliths. High-pressure megacrysts also occur with peridotite xenoliths. Xenolith- and megacryst-bearing calc-alkaline

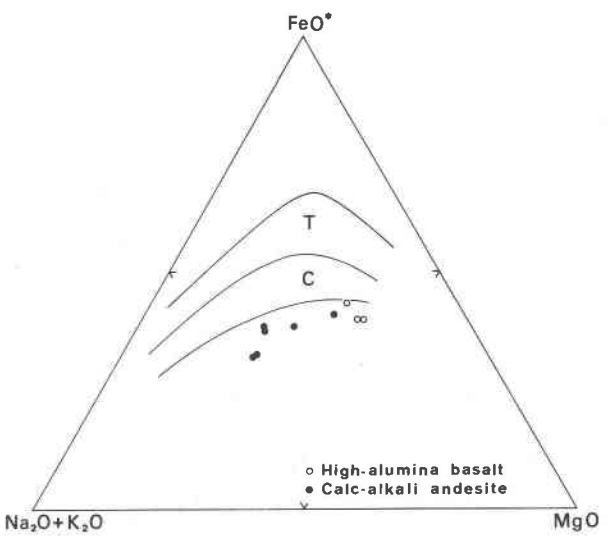

Fig. 3. MgO–FeO* (FeO + Fe_2O_3)–Na_2O + K_2O diagram. T: differentiation trend of the tholeiite series of Nasu zone, northeastern Japan, C: calc-alkaline series of Nasu zone (Kawano and Aoki, 1960; Kawano *et al.*, 1961).

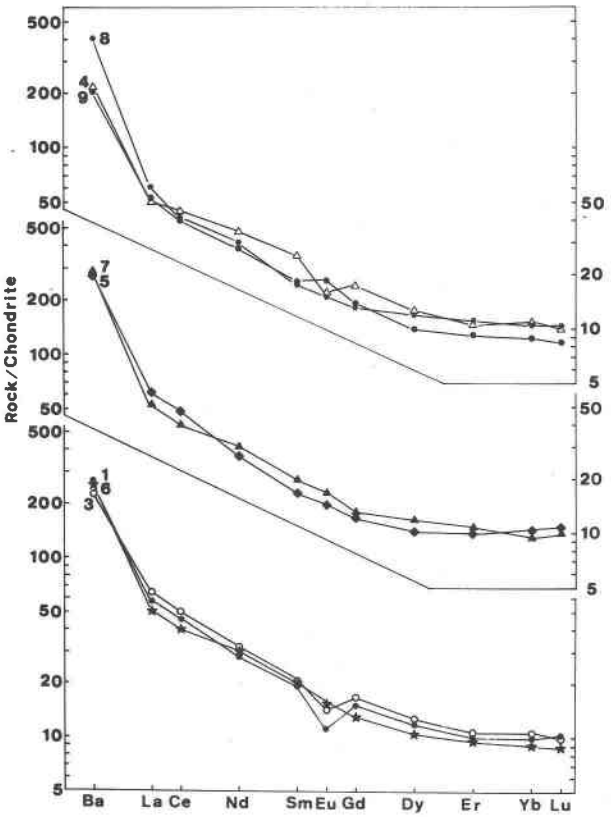

Fig. 4. Chondrite-normalized (Leedey chondrite in Table 2) plot of Ba and REE contents. Numbers are the same as those for Table 1.

andesites have only been found in Itinome-gata volcano and nowhere else in the world. According to Kuno (1967), Aoki and Shiba (1973a) and Arai and Saeki (1980), Itinome-gata and Sannome-gata peridotite xenoliths are characterized by the presence of calcic plagioclase associated with spinel–pyroxene symplectite without exception, in addition to the ordinary spinel peridotite mineral assemblage, presumably because of the relatively thin crust in this district. Furthermore, Takahashi (1980) has demonstrated that some of the Itinome-gata peridotites do not show single *P/T* conditions of equilibration but record complex thermal histories between 800° C and 1,000° C from long residence time in the upper mantle before transportation to the surface. Estimated thickness of the crust based on petrological and geophysical data is indicated to be about 20 to 25 km. In addition, the depth of the Wadati Benioff zone beneath this district is estimated to be about 150 km by the observation of microearthquakes (Hasegawa *et al.*, 1978).

3. Chemical compositions of basalts are transitional between tholeiite and alkali basalt, and agree well with the nature of high-alumina basalt (Kuno, 1960), whereas the andesites are calc-alkaline. Major components vary rather smoothly from basalt to the most salic andesite without any abrupt change with increasing SiO_2. Chondrite-normalized REE and Ba abundances show no major differences among all the volcanic rocks. Sr^{87}/Sr^{86} ratios are constant at 0.7030–0.7033 for basalt and salic andesite, being lower than those of incorporated peridotites (one peridotite is 0.7030 and three are 0.7044–0.7053), hornblende gabbro (0.7041–0.7048) and pyroxene gabbro (0.7035–0.7039) (Zashu *et al.*, 1980). Furthermore, Tanaka and Aoki (1981) have reported the REE and Ba abundances of nine peridotites, two hornblende gabbros, two pyroxene gabbros, and two amphibolites from Itinome-gata. The REE abundances and normalized patterns of peridotites reflect the degrees of basaltic component extractions; namely, undepleted peridotites have the highest concentration and a convex-upwards pattern, whereas Mg-rich and depleted ones have the lowest concentration and a V-shaped pattern. The patterns of calculated liquid phases extracted from these

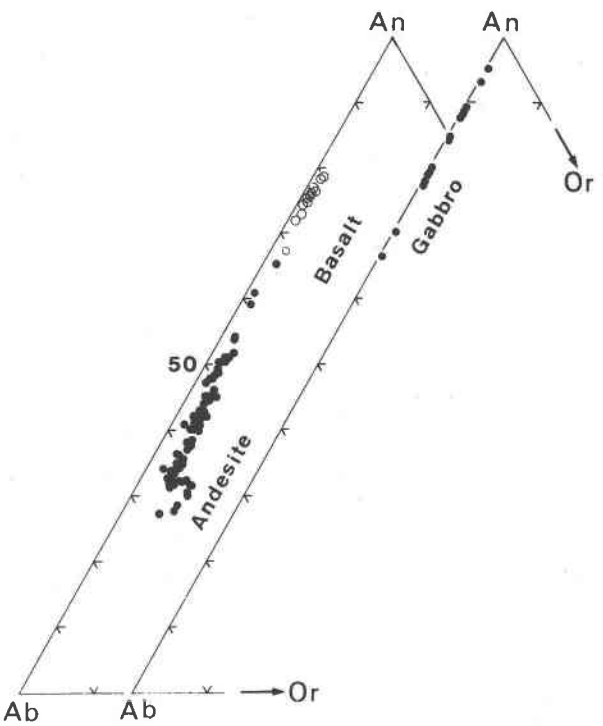

Fig. 5. EPMA analyses of feldspars in mole percent anorthite (An), albite (Ab) and orthoclase (Or). Gabbro: plagioclases in hornblendite-hornblende gabbro xenoliths from Itinome-gata (Aoki, 1971).

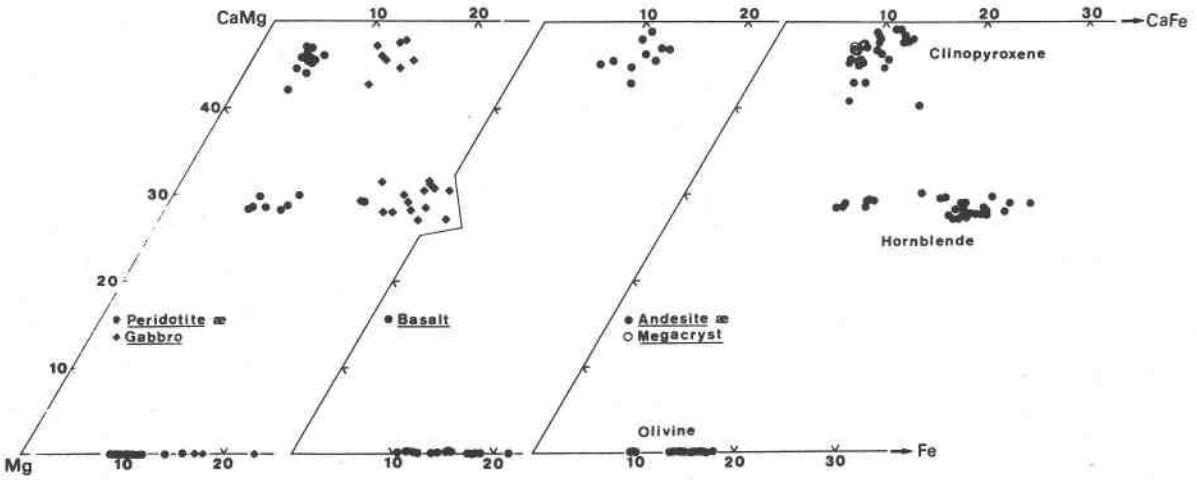

Fig. 6. EPMA analyses of pyroxene, olivine and calciferous amphibole in atomic percent Ca, Mg and Fe. Peridotite: clinopyroxene, olivine and calciferous amphibole in peridotite xenoliths from Itinome-gata (Aoki and Shiba, 1973a, b, 1974b), Gabbro: clinopyroxene, olivine and calciferous amphibole in hornblendite-hornblende gabbro-pyroxene gabbro xenoliths (Aoki, 1971).

peridotites differ from those of the host basalt and andesite and resemble those of island arc, low-alkali tholeiites, which are characterized by LREE-depleted and flat patterns, from the Pacific side of Japan. All the mafic xenoliths have similar tholeiitic patterns. These Sr isotope and REE data indicate no genetic relation between basalt and andesite and their incorporated ultramafic–mafic xenoliths.

Because they contain upper mantle xenoliths, the phenocryst assemblage and chemical compositions of the basalts and salic andesites must have been determined in the uppermost mantle, corresponding to a depth at least 20 to 25 km from the surface. They must have ascended directly and rapidly to the surface without compositional change by fractionation at shallower levels. Furthermore, there is no direct seismologic evidence of partial melting at the subducted oceanic crust (Hasegawa *et al.*, 1978). Accordingly, only two possibilities explain the origin of these Itinome-gata magmas: one is high-pressure fractional crystallization including amphibole fractionation from basalt magma to produce andesite melt, and the other is partial melting of mantle peridotite to produce basalt and andesite magmas under dry and wet conditions, respectively, from the same source region.

Recent experimental work by Allen *et al.* (1975) and Allen and Boettcher (1978) has shown that fractionation of amphibole-bearing silicate phases from basalt magma could be a very effective mechanism for causing SiO_2 increase in the residual melt, without the marked iron concentration that characterizes the tholeiite series (Fig. 3). This concept has been utilized by many petrologists to explain the origin of hornblende-bearing calc-alkaline andesite magmas. For example, the Oshima-Oshima volcano, which is located about 180 km north of Itinome-gata, is composed of 70% alkali basalt and 30% calc-alkaline andesite. Most of the andesites contain abundant xenoliths of hornblende-bearing ultramafic–mafic cumulates. Yamamoto *et al.* (1977) and Mori (1977) have demonstrated that these andesite magmas were formed by amphibole fractionation of alkali basalt magmas at a shallow depth in the upper crust, on the basis of geological and petrographic data. During differentiation of high-alumina basalt magma from the Itinome-gata district, hornblende, biotite, magnetite and plagioclase crystallized in addition to olivine and clinopyroxene; therefore successive liquids should have followed the calc-alkaline trend, as in the case of the Oshima-Oshima basalt–andesite suite, because compositions of subtracted minerals are clearly higher in total FeO, MgO, and CaO and lower in SiO_2, Na_2O, and K_2O than coexisting liquids. Indeed, all the andesites contain these minerals as phenocrysts. Also, Sr^{87}/Sr^{86} ratios are consistent with fractional crystallization including amphibole fractionation.

In order to explain the observed major element variations of the Itinome-gata basalt–andesite suite, degrees of fractional crystallization were calculated using a least-squares mixing computer program

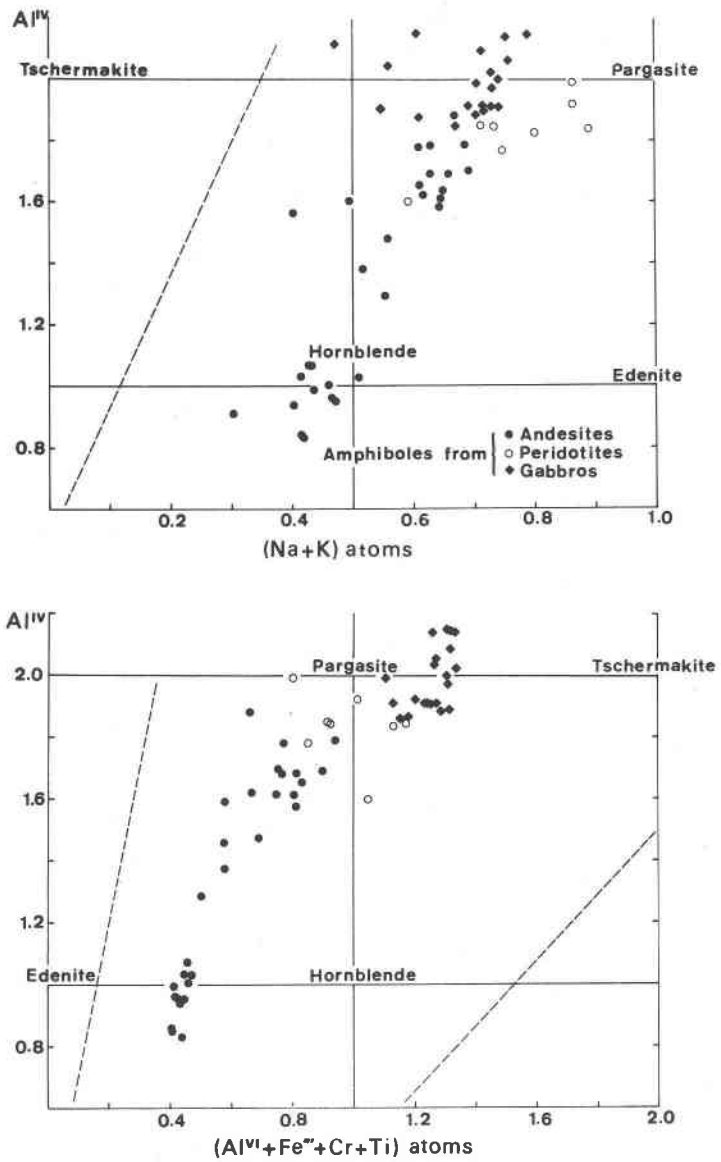

Fig. 7. Plots of calciferous amphibole in Al^{IV}–(Na + K) and Al^{IV}–(Al^{VI} + Fe^{3+} + Cr + Ti) diagram.

(Wright and Doherty, 1970) written by T. Miyata. When hornblende and biotite are included in the calculation, however, the results show a large error implying that hornblende and/or biotite subtraction was minor or negligible. The best-fitting calculations are shown in Table 4. The most mafic and salic andesite liquids can be produced by about 40% and 70% solidification of the least differentiated basalt magma, respectively. Fractional crystallization involving amphibole fractionation cannot, moreover, explain similar REE concentration in all the rocks. This is because the partition coefficient of REE between the sum of subtracted crystals composed of olivine, pyroxene, plagioclase and magnetite with or without hornblende and basalt magma is much less than one (Schnetzler and Philpotts, 1968, 1970). Therefore, it is impossible to subtract these minerals from basalt magma without increasing the REE content of the residual liquids.

When a sequence of magmas is generated by varying degrees of partial melting of peridotite, the REE concentration in magmas varies inversely with degree of melting; namely, with increasing melting of spinel peridotite, total REE concentrations de-

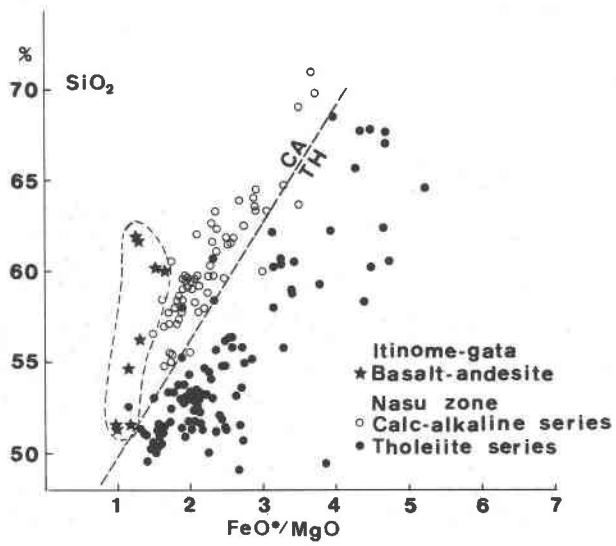

Fig. 8. FeO*/MgO–SiO_2 diagram. Dashed line is the field boundary between tholeiite series and calc-alkaline series (Miyashiro, 1974). Tholeiite series and calc-alkaline series are quoted from Kawano and Aoki (1960) and Kawano *et al.* (1961).

crease rapidly (Shimizu and Arculus, 1975). Accordingly, the same degree of the REE concentration in basalts and andesites can be interpreted as resulting from the same degree of partial melting of the same peridotitic upper mantle.

On the basis of experimental work, Kushiro (1972, 1974), Mysen *et al.* (1974), Kushiro and Sato (1978), and Tatsumi (1981a, b) have demonstrated that calc-alkaline andesite magma can be produced by partial melting of the upper mantle lherzolite under hydrous conditions at depths of 40 to 60 km. Such andesite magmas ought to have higher MgO/total FeO molecular ratio (MgO > FeO) than andesite formed by fractional crystallization of basalt magma, because the former is produced in equilibrium with mantle peridotite which has very high Mg value (about 88 to 90). Indeed, Itinome-gata basalt and andesite contain Mg-rich olivine (Fo_{90-86}) as phenocrysts and also have high MgO/total FeO (1.84–1.15), even in the groundmass composition. According to Roedder and Emslie (1970), the Mg–Fe partition coefficient between olivine and liquid ($D_{Mg-Fe}^{Ol-Liquid}$) is 0.3. The coefficient of these basalts and andesites approaches 0.3, and it is suggested that olivine phenocrysts are nearly in equilibrium with their groundmass. Figure 8 shows the relationship between FeO*/MgO and SiO_2 for Itinome-gata basalt and andesite and for andesite of the tholeiitic series and calc-alkaline series of the Nasu zone. Calc-alkaline andesites of the Nasu zone plot along the boundary line between the tholeiitic series and calc-alkaline series (Miyashiro, 1974); on the other hand, Itinome-gata basalt and andesite plot nearly parallel to the vertical axis, being clearly higher in MgO/FeO* than the calc-alkaline andesites of Nasu zone. Recently, Masuda and Aoki (1979) have demonstrated that the magmas of the tholeiitic series and calc-alkaline series of Nasu zone appear to have been generated by different degrees of partial melting (about 20% and 3% respectively) of the same peridotite upper mantle, based on the Ba, Hf, Th, U and REE content variations. However, there are conspicuous differences between calc-alkaline andesites from Itinome-gata district and those of Nasu zone: the former have clearly higher K_2O, Ba and REE concentrations and Nd^{143}/Nd^{144} and lower Sr^{87}/Sr^{86} ratios, indicating that different source materials are required in these two regions (Kawano *et al.*, 1961; Masuda and Aoki, 1979; Zashu *et al.*, 1980; Nohda and Wasserburg, 1981; Tanaka and Aoki, 1981).

It may be reasonable to consider that calc-alkaline andesite and high-alumina basalt magmas of Itinome-gata district were generated independently by the same degree of partial melting of hydrous and less hydrous parts of the same peridotitic source material which is enriched in LREE and/or depleted in HREE (Lopez-Escobar *et al.*, 1977; Tanaka and Aoki, 1981), at depths greater than those of incorporated peridotite xenoliths, but far above the Wadati-Benioff zone, or the order of 40 to 60 km deep. When it is assumed that the major part of K_2O, F and H_2O are derived from phlogopite, a qualitative estimate of the original H_2O in basalt magmas can be inferred from both F and K_2O contents (Aoki *et al.*, 1981). Estimated H_2O content in the Itinome-gata basalts (K_2O 1.3–1.4% and F 280–290 ppm) is about 0.5 to 0.9%, and that of the andesites would be much higher. Recent experi-

Table 4. Representative results of computer calculation based on 10 major elements for fractional crystallization model

Basalt (No. 1)*	1	Mafic andesite (No. 4)	1
Mafic andesite (No. 4)	0.6084	Salic andesite (No. 9)	0.4869
Ol Fo_{88}	0.0603	Ol Fo_{88}	0.0515
Cpx $Wo_{45}En_{47}Fs_8$	0.0839	Cpx $Wo_{46}En_{42}Fs_{12}$	0.1463
Pl An_{54}	0.2224	Pl An_{54}	0.2596
Mt $Ulvosp_8$	0.0233	Mt $Ulvosp_8$	0.0420
Sum of squares of residuals	0.1142	Sum of squares of residuals	1.1580

* Numbers are the same as those of Table 1.

mental results (Tatsumi, 1981a, b) indicate that the melt of the high magnesian andesite can be in equilibrium with magnesian olivine and pyroxene in the temperature range between 1,000° and 1,100° C and in the pressure range between 10 and 15 kbar in the presence of about 5–20 percent H_2O in the liquid, being presumably produced by 10 percent partial melting of peridotite containing less than 1 percent H_2O. Accordingly, the source materials would be a pargasite-bearing spinel peridotite in which phlogopite is present as the primary or as a metasomatized phase. Some Mg-rich olivine and clinopyroxene, which are sometimes recognized as megacrysts, would be separated from these basalt and andesite magmas (less than 10%) during their upward movement before they reached the top of mantle. Furthermore, the andesite magmas crystallized plagioclase, hornblende, biotite and magnetite with or without quartz in addition to olivine and clinopyroxene, but effective fractionation of these minerals to yield drastic change of residual liquid did not take place at depths of about 30 km. Subsequently, the magmas captured fragments of wall rocks in the upper mantle and lower crust during their rapid ascent to the surface. This hypothesis can explain all the petrographic, mineralogic, and major and trace element geochemical evidence of basalt and andesite from Itinome-gata district.

Acknowledgments

The authors are grateful to Prof. R. Brousse for his helpful discussions. This petrographic and geochemical study was carried out at the Tohoku University, and the manuscript completed at the Université de Paris-Sud during the senior author's tenure of a Fellowship from Ministere des Universites, France. A part of expenses of this study was defrayed with a Grant-in-Aid for Special Project Research (Nos. 420901 and 520102) from the Ministry of Education, Science and Culture of Japan.

References

Allen, J. C., Boettcher, A. L. and Marland, G. (1975) Amphiboles in andesite and basalt: I. Stability as a function of P–T–fO_2. American Mineralogist, 60, 1069–1085.

Allen, J. C., Boettcher, A. L. (1978) Amphiboles in andesite and basalt: II. Stability as a function of P–T–fH_2O–fO_2. American Mineralogist, 63, 1074–1087.

Allen, J. C., Modreski, P. J., Haygood, C. and Boettcher, A. L. (1972) The role of water in the mantle of the Earth: The stability of amphiboles and micas. Proc. 24th Int. Geol. Congr., Sec. 2, 231–240.

Aoki, K. (1971) Petrology of mafic inclusions from Itinome-gata, Japan. Contributions to Mineralogy and Petrology, 30, 314–331.

Aoki, K. (1978) Petrography of Quaternary volcanic rocks in Japan. In I. Kushiro and S. Aramaki Eds., Materials Science of the Earth, II. Igneous rocks and Their Origin, p. 153–170. Iwanami-Shoten, Tokyo (in Japanese).

Aoki, K., Ishikawa, K. and Kanisawa, S. (1981) Fluorine geochemistry of basaltic rocks from continental and oceanic regions and petrogenetic application. Contributions to Mineralogy and Petrology, 76, 53–59.

Aoki, K. and Shiba, I. (1973a) Pyroxenes from lherzolite inclusions of Itinome-gata, Japan. Lithos, 6, 41–51.

Aoki, K. and Shiba, I. (1973b) Pargasites in lherzolite and websterite inclusions from Itinome-gata, Japan. Journal of Japanese Association of Mineralogy, Petrology and Economic Geology, 68, 303–310.

Aoki, K. and Shiba, I. (1974a) Petrology of websterite inclusions of Itinome-gata, Japan. Science Report of Tohoku University, Series, 3, 12, 395–417.

Aoki, K. and Shiba, I. (1974b) Olivines from lherzolite inclusions of Itinome-gata, Japan. Geological Society of Japan Memoir, 11, 1–10.

Arai, S. and Saeki, Y. (1980) Ultramafic-mafic inclusions from Sannomegata crater, Oga peninsula, Japan, with special reference to the Ichinomegata inclusions. Journal of the Geological Society of Japan, 86, 705–708.

Boettcher, A. L. (1973) Volcanism and orogenic belts—the origin of andesites. Tectonophysics, 17, 223–240.

Deer, W. A., Howie, R. A. and Zussman, J. (1963) Rock Forming Minerals, Vol. 2, Chain Silicates. Longmans, London.

Fujimaki, H. and Aoki, K. (1980) Quantitative microanalyses of silicates, oxides and sulfies using an energy-dispersive type electron probe. Science Report of Tohoku University, Series 3, 14, 261–268.

Green, T. H. and Ringwood, A. E. (1968) Genesis of the calc-alkaline igneous rock suite. Contributions to Mineralogy and Petrology, 18, 105–162.

Hawegawa, A., Umino, N. and Takagi, A. (1978) Double-planed structure of the deep seismic zone in the northeastern Japan arc. Tectonophysics, 47, 43–58.

Jakes, P. and Gill, J. B. (1970) Rare earth elements and the island arc tholeiitic series. Earth and Planetary Science Letters, 9, 17–28.

Katsui, Y. and Nemoto, S. (1977) On the ejecta from Itinomegata volcano, Oga peninsula. (Abstr.) Journal of Volcanological Society of Japan, 22, 88 (in Japanese).

Katsui, Y., Yamamoto, S., Nemoto, S. and Niida, K. (1979) Genesis of calc-alkalic andesites from Oshima-Oshima and Ichinomegata volcanoes, north Japan. Journal of Faculty of Science, Hokkaido University, Series, 4, 19, 157–168.

Kawano, Y. and Aoki, K. (1960) Petrology of Hachimantai and surrounding volcanoes, northeastern Japan. Science Report of Tohoku University, Series, 3, 6, 409–429.

Kawano, Y., Yagi, K. and Aoki, K. (1961) Petrography and petrochemistry of the volcanic rocks of Quaternary volcanoes of northeastern Japan. Science Report of Tohoku University, Series, 3, 7, 1–49.

Kuno, H. (1960) High-alumina basalt. Journal of Petrology, 1, 121–145.

Kuno, H. (1967) Mafic and ultramafic nodules from Itinomegata, Japan. In P. J. Wyllie Ed., Ultramafic and Related Rocks, p. 337–342. Wiley, New York.

Kuno, H. and Aoki, K. (1970) Chemistry of ultramafic nodules and their bearing on the origin of basaltic magmas. Physics of Earth and Planet Interiors, 3, 273–301.

Kushiro, I. (1972) Effect of water on the composition of magmas formed at high pressures. Journal of Petrology, 13, 311–334.

Kushiro, I. (1974) Melting of hydrous upper mantle and possible generation of andesitic magma: an approach from synthetic system. Earth and Planetary Science Letters, 22, 294–299.

Kushiro, I. and Sato, H. (1978) Origin of some calc-alkalic andesites in the Japanese islands. Bulletin Volcanologique, 41, 576–585.

Kushiro, I., Yoder, H. S., Jr. and Nishikawa, M. (1968) Effect of water on the melting of enstatite. Geological Society of America Bulletin, 79, 1635–1692.

Lopez-Escobar, L., Frey, F. A. and Vergara, M. (1977) Andesites and high-alumina basalts from the central-south Chile High Andes: Geochemical evidence bearing on their petrogenesis. Contributions to Mineralogy and Petrology, 63, 199–228.

Masuda, A., Nakamura, N. and Tanaka, T. (1973) Fine structures of mutually normalized rare-earth patterns of chondrites. Geochimica et Cosmochimica Acta, 37, 239–248.

Masuda, Y. and Aoki, K. (1979) Trace element variations in the volcanic rocks from the Nasu zone, northeast Japan. Earth and Planetary Science Letters, 44, 139–149.

Miyashiro, A. (1974) Volcanic rock series in island arcs and active continental margins. American Journal of Science, 274, 321–355.

Mysen, B. O., Kushiro, I., Nicholls, I. A. and Ringwood, A. E. (1974) A possible mantle origin for andesitic magmas: discussion on a paper by Nicholls and Ringwood. Earth and Planetary Science Letters, 21, 221–229.

Mori, T. (1977) Genesis of calcalkaline andesites as demonstrated by the examples at Oshima-Oshima and other areas. Journal of Volcanological Society of Japan, 22, 189–200 (in Japanese with English abstract).

Nakamura, N. (1974) Determination of REE, Ba, Fe, Mg, Na and K in carbonaceous and ordinary chondrites. Geochimica et Cosmochimica Acta, 38, 757–775.

Nohda, S. and Wasserburg, G. J. (1981) Nd and Sr isotopic study of volcanic rocks from Japan. Earth and Planetary Science Letters, 52, 264–276.

Ringwood, A. E. (1974) The petrological evolution of island arc systems. Journal of Geological Society of London, 130, 183–204.

Roeder, P. L. and Emslie, R. F. (1970) Olivine–liquid equilibrium. Contributions to Mineralogy and Petrology, 29, 275–289.

Shimizu, N. and Arculus, R. J. (1975) Rare earth element concentrations in a suite of basanitoides and alkali olivine basalts from Grenada, Lesser Antilles. Contributions to Mineralogy and Petrology, 50, 211–240.

Schnetsler, C. C. and Philpotts, J. A. (1968) Partition coefficients of rare-earth elements and barium between igneous matrix and rock forming mineral phenocrysts. In L. H. Ahrens Ed., Origin and Distribution of the Elements. p. 928–938. Pergamon, London.

Schnetzler, C. C. and Philpotts, J. A. (1970) Partition coefficients of rare earth elements between igneous matrix material and rock forming mineral phenocrysts, II. Geochimica et Cosmochimica Acta, 34, 331–340.

Takahashi, E. (1978) Petrologic model of the crust and upper mantle of the Japanese Island arcs. Bulletin Volcanologique, 41, 529–547.

Takahashi, E. (1980) Thermal history of lherzolite xenoliths—I. Petrology of lherzolite xenoliths from the Ichinomegata crater, Oga peninsula, northeast Japan. Geochimica et Cosmochimica Acta, 44, 1643–1658.

Tanaka, T. and Aoki, K. (1981) Petrogenetic implications of REE and Ba data on mafic and ultramafic inclusions from Itinome-gata, Japan. Journal of Geology, 89, 369–390.

Tatsumi, Y. (1981a) Origin of high magnesian andesite. (Abstr.) Geological Society of Japan Abstracts with Programs, 37–38 (in Japanese).

Tatsumi, Y. (1981b) Melting experiments on a high magnesian andesite. Earth and Planetary Science Letters, 54, 357–365.

Wright, T. L. and Doherty, P. C. (1970) A linear programming and least squares computer method for solving petrologic mixing problems. Geological Society of America Bulletin, 81, 1995–2008.

Yamamoto, M., Katsui, Y. and Niida, K. (1978) Petrology of volcanic rocks and ultramafic-mafic inclusions of Oshima-Oshima volcano. Journal of Volcanological Society of Japan, 22, 241–248 (in Japanese with English abstract).

Zashu, S., Kaneoka, I. and Aoki, K. (1980) Sr isotope study of mafic and ultramafic inclusions from Itinome-gata, Japan. Geochemical Journal, 14, 123–128.

Manuscript received, January 12, 1981;
accepted for publication, August 21, 1981.